Sadia Sadiq* and Corinna Harmening

Investigating the potential of stochastic relationships to model deformations

https://doi.org/10.1515/jag-2025-0031
Received February 21, 2025; accepted March 11, 2025;
published online April 24, 2025

Abstract: Terrestrial Laser Scanning (TLS) has proven to be an advanced method for areal deformation analysis, offering high-resolution, contactless data acquisition by capturing millions of data points on a structure's surface. To deterministically model deformations based on subsequently acquired point clouds, corresponding data points are usually required. In order to avoid the cumbersome construction of these corresponding points, this paper aims to enhance TLS-based deformation analysis by further developing a stochastic modeling approach. The main concept of the approach is to model the measured object by means of three components using a collocation-based approach: trend (undistorted object), signal (deformation), and noise (measurement noise). To demonstrate the ability of stochastic relationships to describe deformations, typical temporal deterministic deformation processes, like step, impulse, linear, and periodic responses are simulated by means of non-stationary stochastic processes in this contribution. To accurately model deformation patterns, different types of non-stationary Gaussian temporal processes such as locally stationary, piecewise stationary, and modulated stochastic processes are investigated with respect to their ability to represent typical deformation patterns. When modeling deformations in TLS point clouds as correlated stochastic processes, it is essential to distinguish the correlated deformation signal from the correlated measurement noise. Filtering techniques are employed to separate correlated noise from the deformation signal. Although the proposed method effectively separates signal and noise, the filtering results greatly influence the deformation model results. Future research will focus on alternative solutions for seperating correlated signal and noise and extending the methodology to spatio-temporal point clouds, enabling a more comprehensive analysis of deformations in complex structures across both temporal and spatial dimensions.

Keywords: terrestrial laser scanning; deformation modeling; separation of stochastic processes

1 Introduction

The investigations conducted in this paper are part of the research unit "Deformation analysis based on terrestrial laser scanner measurements" (TLS-Defo) funded by the German Research Foundation (DFG). It aims at addressing the challenges of terrestrial laser scanning (TLS) based monitoring of infrastructure in distinguishing actual geometric changes from uncertainties introduced by the measurement procedure and data processing methods.

TLS has emerged as an essential tool for assessing surface deformation, providing high-resolution, non-invasive data acquisition that captures millions of 3D points from a structure's surface. This capability allows TLS to detect small deformations, which contributes to its extensive use in monitoring structural health [1], identifying landslides [2], and in the field of geotechnical engineering [3]. However, the need for accurate point correspondences between sequential point clouds from different scanning epochs and the analysis of TLS data poses various difficulties, particularly in utilizing TLS for deformation analysis [4].

Despite of the challenges, there are various solutions to use TLS for deformation monitoring, as highlighted in the literature. These include parameter-based comparisons of approximating surfaces, e.g., for the detection of temperature-induced deformation of masonry structures [5]. Aichinger and Schwieger [6] proposed using B-splines to detect small deformations from TLS data across epochs based on curvature parameters, while also highlighting the critical role of scanning parameters like distance and the need for stochastic models to improve accuracy. Yang et al. [7] addressed challenges in 3D point cloud registration for deformation monitoring, introducing efficient methods like piecewise-ICP for targetless registration, super voxel-based segmentation, and identification of stable areas for accurate alignment and deformation detection in complex scenarios.

As can be seen from the state of the art, usually functional descriptions are used to model the deformation.

***Corresponding author: Sadia Sadiq**, Geodetic Institute, Karlsruhe Institute of Technology, Englerstraße 7, 76131 Karlsruhe, Germany, E-mail: sadia.sadiq@kit.edu. https://orcid.org/0009-0008-2168-3310
Corinna Harmening, Geodetic Institute, Karlsruhe Institute of Technology, Englerstraße 7, 76131 Karlsruhe, Germany,
E-mail: corinna.harmening@kit.edu

As an alternative approach, this paper investigates the capabilities of stochastic modeling to describe deformation patterns found in TLS point clouds. The fundamental idea behind this approach is to model the acquired point clouds with a least squares collocation (LSC)-like approach through three superimposing parts: trend (which represents the undistorted object), signal (which captures the deformation), and noise (resulting from measurement uncertainties) [8].

With the stochastic signal representing the deformation, two research questions arise:

1) Which types of stochastic processes are usable to pursue the approach? To answer this question, typical deformation patterns are simulated by means of different types of stochastic processes. The investigation regarding the potential of stochastic processes to model deformations is restricted to the example of 1D time series in this paper, but will be extended to the spatio-temporal domain to improve the deformation model proposed by Harmening and Neuner [8] in future.
2) How can the two stochastic parts, the signal and the noise, be separated, especially in case both parts are correlated? For this purpose, different low-pass filters are investigated with respect to their ability to separate the two stochastic quantities. The approaches are evaluated by means of simulated data.

The paper is structured as follows: Section 2 covers the mathematical foundations essential for the development of the proposed approach. In Section 3, the investigation of stochastic processes for deformation modeling is presented, where different types of deformation are analyzed. Further, Section 4 focuses on the development and application of a strategy to separate signal and noise, specifically addressing the separation of correlated noise from the correlated signal. Finally, Section 5 concludes the paper and provides an outlook for future research directions.

2 Mathematical basics

2.1 Deterministic deformation processes

A change in the acting forces causing deformation is typically categorized into four main types: (a) step (abrupt) (b) impulse (c) periodic or (d) linear changes. The system's response to these forces can be described as the solution of a first-order differential equation, capturing the temporal relationship between the acting forces $x(t)$ and the resulting deformation $y(t)$. These responses are mathematically modeled as follows [9–11]:

$$\Delta y(t) = \begin{cases} H_\infty \left(1 - e^{-\frac{t-t_0}{T}}\right) \Delta x(t_0) & \text{(a)} \\ H_\infty \left(\frac{1}{T} e^{-\frac{t-t_0}{T}}\right) \Delta x(t_0) & \text{(b)} \\ H_\infty \left(\frac{A}{\sqrt{\omega^2 T^2 + 1}} \sin(\omega t + \Phi)\right) \Delta x(t_0) & \text{(c)} \\ H_\infty \left(\frac{1}{1 + e^{-\frac{t-t_0}{T}}}\right) \Delta x(t_0) & \text{(d)} \end{cases} \tag{1}$$

where:

H_∞: system-specific constant represents the steady-state gain of the system,

T: time constant,

$\Delta x(t_0)$: change in the acting force $x_2 - x_1$ at time t_0,

A: amplitude of periodic force,

ω: angular frequency of periodic variation,

Φ: phase shift due to inertia, determined by the time constant T and the forcing ω.

Figure 1 illustrates how the system adapts over time to different force types. A step response (equation (1a)), represented by the blue curve, occurs when the force abruptly changes [9]. Impulse response (equation (1b)) as shown in red, describes a sharp, brief force applied at a single moment, causing a deformation [9]. Periodic response (equation (1c)) illustrated by the green curve, results from forces that repeat over time, causing oscillations in deformation, typical in cyclic loading systems ([10]; p. 18 ff.). Linear response (equation (1d)) depicted by the purple curve, corresponds to forces that change gradually over time, such as temperature variations or smooth load increases [11].

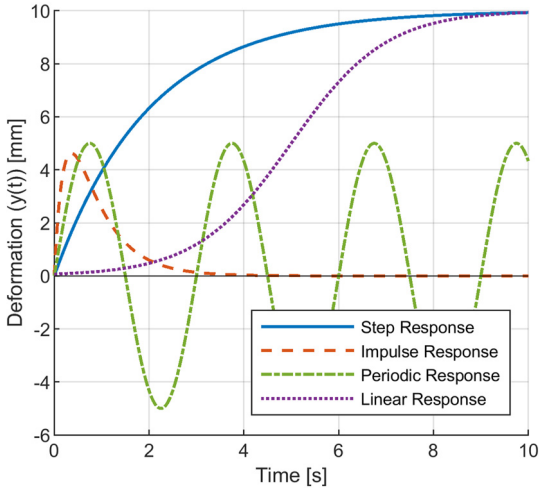

Figure 1: System responses corresponding to different acting forces.

These responses help engineers to predict the behavior of structures under varying loads, stresses, and environmental conditions.

2.2 Gaussian stochastic processes

A *temporal stochastic process* is a collection of random variables $Z(t)$, where each realization represents a possible outcome of the studied phenomenon ([12]; p. 110). A *Gaussian stochastic process* is completely defined by its first two statistical moments: its expectation value $\mu(t)$ and its covariance function $C(t_1, t_2)$ ([13], p. 95 ff.):

$$\mu(t) = \mathbb{E}[Z(t)] \tag{2}$$

$$\mathrm{C}(t_1, t_2) = \mathbb{E}[(Z(t_1) - \mu(t_1))(Z(t_2) - \mu(t_2))] \tag{3}$$

where:

(t_1, t_2): points in the temporal domain,

$\mathbb{E}[\ ]$: the expectation value.

The covariance function in equation (3) is a generalization of the process variance ([14]; p. 343):

$$C(t, t) = \mathrm{Var}\{Z(t)\} = \sigma^2(t). \tag{4}$$

The autocorrelation function, using variances at t_1 and t_2, is ([13], p. 95 ff.):

$$\rho(t_1, t_2) = \frac{C(t_1, t_2)}{\sqrt{\sigma^2(t_1)\sigma^2(t_2)}} \tag{5}$$

Gaussian stochastic processes are *non-stationary*, when their moments vary with time and *stationary*, when their statistical properties are constant over time ($\mu(t) = \mu, \sigma^2(t) = \sigma^2$). For stationary processes, the covariance depends only on the time lag $\tau = t_2 - t_1$: $C(t_1, t_2) = C(\tau)$.

2.2.1 Types of non-stationary Gaussian processes

A process is *locally stationary* if its covariance function $C(t_1, t_2)$ can be expressed as the product of time-dependent variances and a correlation function depending on the temporal distance τ [15]:

$$C(t_1, t_2) = \sigma_\mu(t_1)\sigma_\mu(t_2)\rho_\Delta(\tau). \tag{6}$$

A *modulated stationary process*, as a special case of locally stationary processes, introduces non-stationarity by modulating a stationary correlation function $\rho(\tau)$ with a deterministic function $q(t)$ [16]:

$$C(t_1, t_2) = q(t)\rho(\tau). \tag{7}$$

For processes exhibiting complex behavior, *piecewise stationary processes* simplify analysis by treating the process as stationary within small intervals $[t_i, t_{i+1}] \subseteq T$ [17]:

$$C(t_1, t_2) = C(\tau), \quad t_1, t_2 \in [t_i, t_{i+1}] \tag{8}$$

$$\mu(t) = \mu, \quad t \in [t_i, t_{i+1}]. \tag{9}$$

2.2.2 Simulating observations as a realization of a stochastic process

When stochastically simulating observations as a realization of a stochastic process, the starting point is a time series vector $\mathbf{Z} = (Z(t_1), \ldots, Z(t_n))^T$ of uncorrelated random variables $\mathbf{Z} \sim \mathcal{N}(0, \mathbf{I})$. A positive semidefinite covariance function $C(\tau)$ forms the covariance matrix $\mathbf{\Sigma}$:

$$\mathbf{\Sigma} = \begin{bmatrix} C(t_1, t_1) & C(t_1, t_2) & \ldots & C(t_1, t_n) \\ C(t_2, t_1) & C(t_2, t_2) & \ldots & C(t_2, t_n) \\ \vdots & \vdots & \ddots & \vdots \\ C(t_n, t_1) & C(t_n, t_2) & \ldots & C(t_n, t_n) \end{bmatrix}. \tag{10}$$

To generate a correlated time series $\mathbf{X}$, the Cholesky decomposition $\mathbf{\Sigma} = \mathbf{R}^T\mathbf{R}$ is used to transform the random variable $\mathbf{Z}$ into a normally distributed and correlated random variable $\mathbf{X} \sim \mathcal{N}(\boldsymbol{\mu}, \mathbf{\Sigma})$ as follows ([18], p. 167):

$$\mathbf{X} = \mathbf{R}^{\mathrm{T}}\mathbf{Z} + \boldsymbol{\mu}. \tag{11}$$

2.3 A collocation-based deformation model for laser scanning point clouds

The deformation model applied in this publication builds upon [8] and is based on the ideas of a least squares collocation (LSC) ([19]; p. 99 ff.). Thus, the observations $\boldsymbol{l}$ are represented as the sum of the deterministic trend $\boldsymbol{Ax}$, which provides a rough approximation of the observations, the stochastic signal $\mathbf{s}$, which carries the phenomenon's information through stochastic relationships, and the measurement noise $\boldsymbol{\varepsilon}$, which accounts for the uncertainty inherent in the measurement process [8]:

$$\mathbf{l} = \mathbf{Ax} + \mathbf{s} + \boldsymbol{\varepsilon}. \tag{12}$$

Both, the signal and the noise are assumed to follow normal distributions with an expectation value of zero and covariance matrices of signal $\mathbf{\Sigma}_{\mathbf{ss}} = \sigma_0^2\mathbf{Q}_{\mathbf{ss}}$ and noise $\mathbf{\Sigma}_{\boldsymbol{\varepsilon\varepsilon}} = \sigma_0^2\mathbf{Q}_{\boldsymbol{\varepsilon\varepsilon}}$, respectively. Additionally, it is assumed that there are no correlations between the signal and the noise ([14]; p. 206). Following the basic model of LSC in equation (12), in the deformation model, the trend repre-

sents the object's initial and undistorted shape, which is captured during the first measurement epoch. Hence, the trend is estimated once and then subtracted from the original data. That means that any deformation is described by the stochastic signal only. In the original model [8], the signal is assumed to be a realization of a locally stationary process (cf. Section 2.2.2). The estimation of the signal, therefore, requires the following steps: (1) trend estimation and subtraction, (2) detection of distorted regions, (3) clustering and normalization to establish stationarity, (4) estimating of covariance functions to establish $\mathbf{\Sigma}_{ss}$, (5) estimation of the signal.

3 Investigation of stochastic processes for deformation modeling

To justify the use of a stochastic approach, initially, typical deformation processes are modeled stochastically, verifying that – vice versa – deformation can be modeled by means of stochastic relationships. Although laser scanning point clouds are usually three-dimensional, these initial investigations conducted in this paper are restricted to 1D time series and will be extended to 4D (space and time) data sets in the future.

3.1 Theoretical considerations

Non-stationary stochastic processes are ideal for describing deformation, as they capture the high variability in magnitude across deformed areas and observation periods. However, estimating their moments poses a significant challenge in data modeling. By limiting non-stationarity within well-structured frameworks – for example, piecewise or smoothly modulated processes – it becomes possible to estimate stochastic moments while maintaining the flexibility of non-stationary processes.

Locally stationary processes, with their stationary correlation structures and slowly varying variances, can model continuous deformation patterns effectively while maintaining computational efficiency [8]. This study extends the foundation established by Harmening and Neuner [8] by incorporating the piecewise and modulated stochastic processes. These approaches address the shortcomings of locally stationary models in representing discontinuous deformation patterns and deformation patterns with changing characteristics. Piecewise processes, for example, allow abrupt changes in deformation behavior, which makes them especially well suited to modeling transitions between boundaries or regions with contrasting physical properties [20]. On the other hand, modulated stochastic processes allow to incorporate functional knowledge into the stochastic description and, hence, represent a middle way between a purely functional and a purely stochastic description of a deformation pattern.

3.2 Simulation of temporal deformation processes using stochastic relationships

In order to empirically support the considerations formulated above, different types of stochastic processes are used here to simulate the typical deformation patterns introduced in Section 2.1. For this purpose, simulated correlated time series of all four deformation processes are generated as described in Section 2.2.2. Specifically, positive definite exponential correlation functions of type:

$$C(\tau) = e^{-b|\tau|}, \quad b > 0 \tag{13}$$

are used, where b determines the rate of exponential decay and is associated with the correlation length. A small value of b indicates a stronger correlation in the signal, resulting in a less pronounced stochastic behavior within the time series. As only large correlation lengths can produce quasi-deterministic deformation patterns [8], a small value $b = 0.000005$ is used for the following investigations.

In order to receive a deformation pattern in the simulated time series, the stationary correlation function is transformed into a non-stationary covariance function by using temporally varying variances $\sigma(t)^2$. Among the four deterministic processes discussed in Section 2.1, the step response is used as an example to illustrate the evolution of deformation behavior under changing stochastic conditions.

Figure 2 illustrates the stochastically simulated system's step response over time, presenting both the uncorrelated $\mathbf{Z}$ (blue dots) and correlated data points $\mathbf{X}$ (red line) in equation (11) with an expectation value of zero. Initially, the deformation follows a stationary process with constant variance. At $t \approx 500$ s it transitions into a modulated stochastic process (equation (7)). For the modulation of the variance, the functional description of the step response (equation 1(a)) is used. This causes the variance to increase with time, reflecting external influences on the system's response. This modulation introduces a time-varying variance, making the process non-stationary. By the end, the deformation stabilizes, with

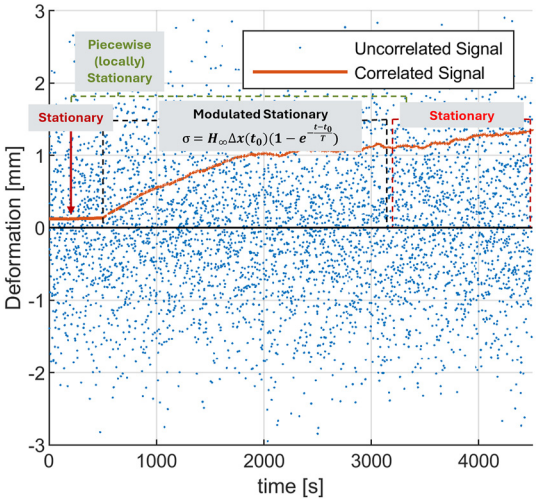

Figure 2: Step response as a realization of different types of stochastic processes ($H_\infty = 1, T = 1$).

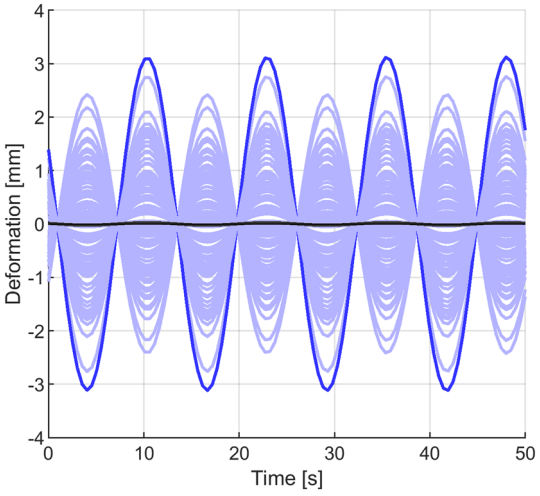

Figure 4: Several realizations of a periodic response (blue curves) and the ensemble average (black), indicating an expectation value of zero.

the variance becoming constant at $t \approx 3{,}100$ s, indicating adaptation to external forces. Due to the separation into several intervals, the entire process is a piecewise (locally) stationary process.

The methodology for the step response can be extended to other deformation processes, such as impulse, periodic, and linear responses, as shown in Figure 3, by modulating the variance with different deterministic functions (equation (1)). The type of deformation is controlled by the variance level's behavior. While only the exponential correlation function (equation (13)) is used in this study, further investigations regarding the influence of the type of correlation function will be done in the future.

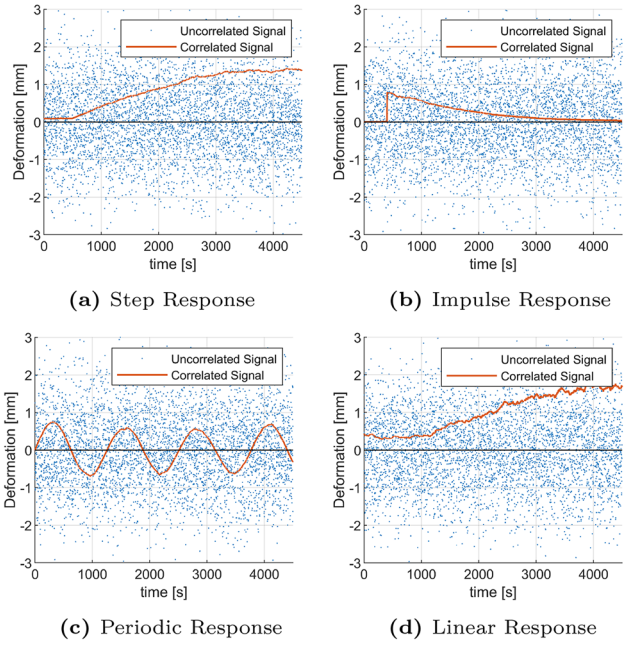

Figure 3: Stochastic simulation of typical temporal deformation processes.

In the context of the stochastic deformation model introduced in Section 2.3, a stationary expectation value of zero is a prerequisite for the validity of the respective formulas. This assumption indicates that, on average, no deformation occurs, which is consistent with the null hypothesis of the congruency model ([14]; p. 252). For each realization, a deformation may occur, but over multiple realizations, the mean value is zero. Figure 4 visually illustrates this principle for a periodic response, showing how multiple realizations aggregate to an overall mean of zero and, hence, highlighting the expectation value of zero.

4 Investigations regarding the separation of signal and noise

When modeling deformations as a realization of a stochastic process as described in Section 2.2.2, a crucial step is the separation of the two stochastic parts, the noise (=measurement noise) and the signal (=deformation).

This study begins with the premise that noise typically exhibits higher frequencies compared to the underlying signal, a reasonable assumption for most structures, including dams and bridges [21], acquired by means of a TLS.

Hence, low-pass filters are investigated with respect to their ability to separate noise and signal. The step response is used as an example to demonstrate the operation of the filters and the deformation model. The research is conducted for both white noise and correlated noise, but the results of correlated noise are presented here, as the results are comparable. Figure 5 illustrates the simulated input data, comprising a stochastic signal with a step response (equation (1a)) and correlated noise. The parameter b of the autocorrelation function (equation (13)) governs the behavior of the signal and noise. A weakly correlated noise with a correlation length of $t \approx 5$ s and $b = 0.5$ is chosen, representing high-frequency components. In contrast, the signal is modeled with a large correlation length >200 s and a small value of $b = 0.0000005$, reflecting a highly correlated, low-frequency deformation pattern.

Four different filters are applied as shown in Figure 6: the Butterworth filter [22], the median filter [23], the Savitzky-Golay (linear) filter [24] and the moving average filter [25]. Assuming that the noise characteristics are known due to an appropriate stochastic model, the filter parameters are selected based on the noise's correlation length to effectively suppress the weakly correlated, high-frequency noise.

The filtering results illustrate the ability of the different techniques to reduce noise while preserving the underlying deformation. As shown in Figure 6, the Butterworth filter provides a smooth signal but introduces oscillations due to its frequency-domain characteristics and the effects of the finite signal length, particularly near the boundaries. The median filter effectively removes noise, but it also introduces oscillations which are similar to those caused by the

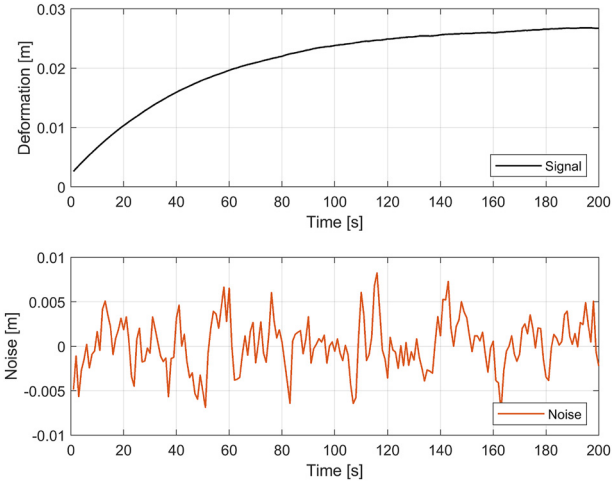

Figure 5: Simulated data.

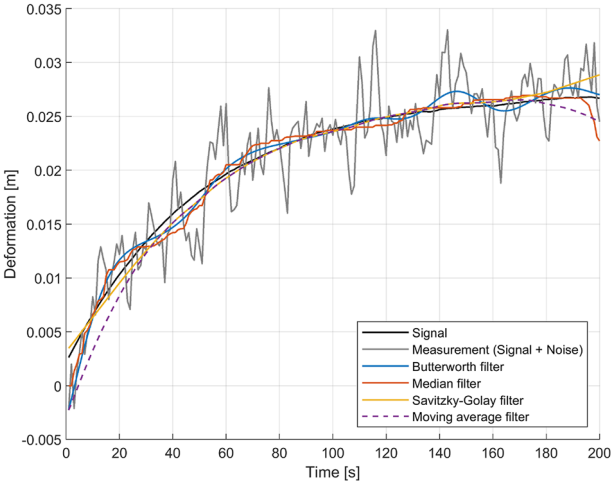

Figure 6: Results of the four filtering approaches for correlated noise using a cutoff frequency of 1/39 Hz or a window size of 39 s, respectively.

Butterworth filter. The Savitzky-Golay filter preserves the signal while smoothing fluctuations, making it most suitable for this application. The moving average filter exhibits a similar smoothing effect but with larger deviation at the beginning and end of the time series.

Table 1 quantitatively compares the averaged absolute discrepancy (AAD) with respect to the known signal for all four filters using forward and forward-backward filtering with three filter lengths. AAD highlights that forward-backward implementations generally improve the filters' accuracy. Among the tested filters, the Savitzky-Golay filter with a window size of 25 s (equaling two times the noise's correlation length) achieves the lowest AAD, indicating the best performance among all investigated filters and successfully separating most parts of the noise from the signal.

The filtered measurements are subsequently used to estimate the signal's covariance structure, forming the basis of the deformation model described in Section 2.3. This process begins with k-means clustering of the time series to identify locally stationary regions. A local variance is estimated using the 3-sigma rule for each cluster. The time series normalized by the variance enables the estimation of the stationary correlation structure. For this purpose, initially, empirical correlograms are estimated. From the correlograms, the autocorrelation function is derived (see [8] for further details).

To establish the stochastic model of the signal, the empirical correlations are approximated using an analytical exponential correlation function (equation (13)), which ensures positive semi-definiteness of the resulting covariance matrix. This function is used to generate the

Table 1: Comparison of different filtering techniques.

Forward filters			Forward-backward filters		
Filter type	**Parameter**	**AAD (mm)**	**Filter type**	**Parameter**	**AAD (mm)**
	Cutoff freq. = 1/13 Hz	1.7349		Cutoff freq. = 1/13 Hz	1.4897
Butterworth	Cutoff freq. = 1/25 Hz	1.6077	Butterworth	Cutoff freq. = 1/25 Hz	0.98763
	Cutoff freq. = 1/39 Hz	1.8863		Cutoff freq. = 1/39 Hz	0.65949
	Window size = 13 s	1.1462		Window size = 13 s	1.0556
Median	Window size = 25 s	0.78232	Median	Window size = 25 s	0.73099
	Window size = 39 s	0.71568		Window size = 39 s	0.67588
	Window size = 13 s	1.0188		Window size = 13 s	0.79116
Savitzky-Golay	Window size = 25 s	0.59132	Savitzky-Golay	Window size = 25 s	0.43474
	Window size = 39 s	0.46263		Window size = 39 s	0.47569
	Window size = 13 s	0.97668		Window size = 13 s	0.78279
Moving average	Window size = 25 s	0.60048	Moving average	Window size = 25 s	0.52291
	Window size = 39 s	0.55229		Window size = 39 s	0.76181

correlation matrix, which is subsequently converted into the covariance matrix $\mathbf{\Sigma}_{ss}$ by incorporating the locally stationary variances.

Finally, the collocation approach, detailed in Section 2.3, is applied to estimate the signal, and hence, the deformation. Figure 7 illustrates the deviations of filtering (using a cutoff frequency of 1/39 s or a window size of 39 s, respectively) and the subsequently performed LSC results from the true deformation signal for all four filters.

Comparing the deviations resulting from the filtering and from LSC, the strong influence of the filtering result on the LSC results becomes obvious: The patterns which are recognizable in the filtering results directly trace into the results of LSC. Particularly striking are the discontinuities that occur in the results of LSC: Here, the effect of the discrete clustering when determining the local variances is clearly visible, making investigations about smooth transitions between the clusters necessary.

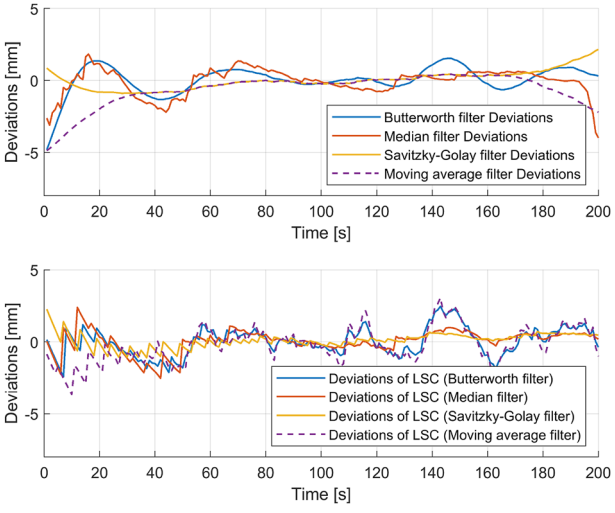

Figure 7: Deviations w.r.t the true signal after filtering (top) and after applying the deformation model (bottom).

Comparing the different filtering approaches, the Butterworth and median filter lead to larger deviations in both filtering and LSC results. Savitzky-Golay and moving average filters provide smaller deviations, making them more suitable for this analysis. The LSC results clearly reduce the noise, as the presented deviations are considerably smaller than 1 mm.

5 Conclusion and outlook

This paper demonstrates the potential of stochastic modeling for capturing deformation patterns in time series. The investigations in this paper reveal that typical deformation patterns like step, impulse, periodic, and linear responses can be described as realizations of non-stationary stochastic Gaussian processes. Yet, as the investigations are currently restricted to the temporal domain, an extension to spatio-temporal point clouds has to be realized in the future.

The proposed approach of separating a correlated signal from correlated noise in time series by using low-pass filtering techniques separates the major part of the noise from the signal. However, as the filtering's results strongly influence the result of the deformation model, it needs refinement. Future work will focus on investigating alternative solutions for signal and noise separation and extending the approach from temporal to spatio-temporal models, enabling a more comprehensive analysis of deformations in complex structures over both time and space.

Acknowledgments: This article presents the results developed during the research project "Deformation Analysis Based on Terrestrial Laser Scanner Measurements (TLS-Defo)" (FOR 5455), which is funded by the Deutsche Forschungsgemeinschaft (DFG): HA 10076/1-1.
Research ethics: Not applicable.
Informed consent: Not applicable.
Author contributions: All authors have accepted responsibility for the entire content of this manuscript and approved its submission.
Use of Large Language Models, AI and Machine Learning Tools: None declared.
Conflict of interest: The authors state no conflict of interest.
Research funding: Deutsche Forschungsgemeinschaft (DFG) -HA 10076/1-1.
Data availability: Not applicable.

References

1. Kaartinen E, Dunphy K, Sadhu A. LiDAR-based structural health monitoring: applications in civil infrastructure systems. Sensors 2022;22:4610.
2. Barbarella M, Fiani M, Lugli A. Landslide monitoring using multitemporal terrestrial laser scanning for ground displacement analysis. Geomatics Nat Hazards Risk 2015;6:398—418.
3. Shen N, Wang B, Ma H, Zhao X, Zhou Y, Zhang Z, et al. A review of terrestrial laser scanning (TLS)-based technologies for deformation monitoring in engineering. Measurement 2023;223:113684.
4. Mukupa W, Roberts GW, Hancock CM, Al-Manasir K. A review of the use of terrestrial laser scanning application for change detection and deformation monitoring of structures. Surv Rev 2017;49:99—116.
5. Ötsch E, Neuner HB. Detektion und Analyse von temperaturbedingter Deformation eines konischen Industrieschlotes. In: Internationalen Ingenieurvermessungskurs. Zürich: Wichmann; 2023:321—34 pp.
6. Aichinger J, Schwieger V. Studies on deformation analysis of TLS point clouds using B-splines — a control point based approach (part I). J Appl Geodesy 2022;16:279—98.
7. Yang Y, Czerwonka-Schröder D, Holst C. Piecewise-ICP: efficient registration of 4D point clouds for geodetic monitoring. Technical report, Copernicus Meetings; 2024.
8. Harmening C, Neuner H. A spatio-temporal deformation model for laser scanning point clouds. J Geod 2020;94:26.
9. Pelzer H. Zur Analyse von permanent registrierten Deformationen. Internationaler Kurs für Ingenieurvermessungen hoher Präzision. Darmstadt, Deutschland: Technische Hochschule Darmstadt; 1976:781—96 pp.
10. Seeler KA. System dynamics: an introduction for mechanical engineers. New York, NY: Springer; 2014.
11. Kyurkchiev N, Markov S. Sigmoid functions: some approximation and modelling aspects: some moduli in programming environment MATHEMATICA. Saarbrücken, Germany: LAP LAMBERT Academic Publishing; 2015.
12. Bendat JS, Piersol AG. Random data: analysis and measurement procedures. Hoboken, NJ, USA: John Wiley & Sons; 2011.
13. Schlittgen R, Streitberg BHJ. Zeitreihenanalyse. München, Deutschland: Oldenbourg (Lehr-und Handbücher der Statistik); 2001.
14. Heunecke O, Kuhlmann H, Welsch W, Eichhorn A, Neuner H. Handbuch Ingenieurgeodäsie, 2nd improved and revised ed. Berlin: Wichmann; 2013.
15. Genton M, Perrin O. On a time deformation reducing nonstationary stochastic processes to local stationarity. J Appl Probab 2004;41:236—49.
16. Dargahi-Noubary GR. A statistical comparison of various source formulations for explosions and earthquakes. J Int Assoc Math Geol 1981;13:119—33.
17. Adak S. Time-dependent spectral analysis of nonstationary time series. J Am Stat Assoc 1998;93:1488—501.
18. Koch KR. Parameterschätzung und Hypothesentests in linearen Modellen. Bonn, Deutschland: Dümmlers; 1997.
19. Moritz H. Advanced physical geodesy, 2nd ed. Karlsruhe: Wichmann; 1989.
20. Last M, Shumway R. Detecting abrupt changes in a piecewise locally stationary time series. J Multivariate Anal 2008;99: 191—214.
21. Pehlivan H. Frequency analysis of GPS data for structural health monitoring observations. Struct Eng Mech 2018;66:185—93.
22. Shouran M, Elgamli E. Design and implementation of Butterworth filter. Int J Innov Res Sci Eng Technol 2020;9: 7975—83.
23. Mertzios BG, Venetsanopoulos AN. Modular realization of multi-dimensional filters. Signal Process 1984;7:351—69.
24. Savitzky A, Golay MJE. Smoothing and differentiation of data by simplified least squares procedures. Anal Chem 1964;36:1627—39.
25. Alessio E, Carbone A, Castelli G, Frappietro V. Second-order moving average and scaling of stochastic time series. Eur Phys J B 2002;27:197—200.